*J. Phys. Chem. A* **2004,** *108,* 1629−1634

# Comparison of Electronic Structure Theories for Solvated Molecules: RISM-SCF versus PCM

**Hirofumi Sato* and Shigeyoshi Sakaki**

*Department of Molecular Engineering, Kyoto University, Yoshida, Kyoto 606-8501, Japan*

*Received: November 13, 2003; In Final Form: December 25, 2003*

Two modern theories that can handle electronic structures of solvated molecules, RISM-SCF and PCM, are compared in a typical $S_N2$ reaction: $Cl^- + CH_3Cl \rightarrow ClCH_3 + Cl^-$. The potentials of mean forces for the reaction in aqueous solution calculated with the two methods are very similar despite the different theoretical standpoint in dealing with solvation effects. However, a new energy-partitioning analysis sheds light on their differences. Both of the electronic structures computed by RISM-SCF and PCM are polarized compared to that from the standard gas-phase computation, but they are slightly different from each other in detail. The polarization of the C−H bond is emphasized in RISM-SCF, but that of the Cl−C bond is dominant in PCM. It is also shown that the change in the electronic structure of the carbon atom is a major cause of the reaction barrier.

## 1. Introduction

In the last two decades, the theory of the electronic structure of solvated molecules has attracted many researchers' attentions, and various types of combination methods have been developed.[1] These can be roughly classified into three categories, namely, the dielectric continuum model, quantum mechanical/molecular mechanics (QM/MM), and method based on the integral equation theory for liquids. The PCM (polarizable continuum model)[2] is obviously one of the most sophisticated achievements in the framework of the dielectric continuum model and is now widely used through many program packages in the field of quantum chemistry. Although the dielectric continuum model including PCM treats solvent molecules in an implicit way, methods in the other two categories are regarded as explicit solvation models. RISM-SCF,[1,3,4] which is a representative of the methods based on the integral equation theory, compiles two ab initio methods in theoretical chemistry: one is the RISM (reference interaction site model),[5,6] and the other is ab initio molecular orbital theory. The method determines the electronic structure as well as the geometry of a solute molecule and the statistical solvent distribution around the solute in a consistent manner. It is a remarkable advantage that the RISM-SCF method can provide information about the microscopic solvation structure based on the statistical mechanics.

All these methods of the electronic structure of solvated molecules have been developed and assessed in terms of linking to experimental knowledge. Hence, agreement with experimental data, especially in solvation energy, is usually the primary concern, and recent theories satisfy these requirements to high accuracy. Even though the agreement in energy is improved, how about the wave function obtained by the method? Moreover, a comparison of the wave functions or energy profiles computed by different solvation models has been rarely examined. Wave functions of solvated molecules computed by different methods should be different from each other.

Considering these circumstances, we report a comparison of the two modern quantum chemical methods for a solvated molecule. A typical $S_N2$ reaction,

$$Cl^- + CH_3Cl \rightarrow ClCH_3 + Cl^-$$

is chosen as the benchmark system, and wave functions computed by PCM and RISM-SCF methods are compared. Numerous studies on the symmetric $S_N2$ reaction in aqueous solution have been reported; these are based on the dielectric continuum model,[7,8] QM/MM,[9] RISM,[10] and classical molecular simulations.[11,12] It is reported in all of them that the reactant and product are strongly stabilized by solvation. Although the energy profile of the reaction shown in the present study is very similar to that in previous studies, details of the event governed by the solute's wave function clearly depend on the methodologies employed to the treat solvation effect. A new energy-partitioning scheme introduced very recently is used to analyze the wave functions.

## 2. Computational Methods

The electronic wave functions were computed on the basis of the RHF method with the 6-311G* basis set.[13] It is known that electron correlation effects do not play any significant role in the present system and that the RHF method is enough to understand the reaction profile. Moreover, the difference in the electron correlation effects between RISM-SCF and PCM due to solvation is a higher-order contribution and beyond the scope of the present study. As the "reaction coordinate" $R$, the difference between the two Cl−CH $_3$ bond lengths was chosen.

$$R = r(Cl-CH_3) - r(CH_3-Cl)$$

The potential energy curve was computed along $R$ by optimizing all of the other degrees of freedom by using the standard ab initio MO method. Computations in the aqueous solution phase were then carried out with the RISM-SCF and PCM methods with these gas-phase geometries because we wish to exclude the contribution of the geometrical difference to the electronic

---

* Corresponding author. E-mail: hirofumi@moleng.kyoto-u.ac.jp.

10.1021/jp0374758 CCC: $27.50

**TABLE 1: Lennard-Jones Parameters**

| | $\sigma$/Å | $\epsilon$/kcal mol$^{-1}$ |
|---|---|---|
| C | 3.83 | 0.18 |
| H | 2.00 | 0.07 |
| Cl | 4.85 | 0.02 |

structure. Note that optimized geometries in the solution phase obtained by the RISM-SCF and PCM methods are generally different, which means that there are several definitions of optimized geometry. By fixing the geometry at the gas-phase optimized structure, we can extract the difference in the electronic structures of the solvated molecule caused only by the difference in the employed methods. We should also address the fact that the geometrical coordinate is not usually suitable as a reaction coordinate to describe chemical reactions in solution, similar in its spirit in the Kramers theory of reaction rates.[9] In other words, the transition state in the solution phase should not be defined as a particular geometry of a solute molecule but as an ensemble of its geometrical structures. However, because we are focusing on the difference between the two methods based on electronic structure theories, the potential of mean force (PMF) and its components are discussed as functions of the traditional coordinate $R$ in the present study. The density of the solvent water was assumed to be 0.033337 molecule/Å$^3$ at 298.15 K. In RISM-SCF theory, a model with all-atom-type interactions including six sites, whose Lennard-Jones parameters were taken from the literature[9,10] and summarized in Table 1, was employed. The SPC-like water[14] was used to describe the solvent. All of the van der Waals interactions between the solute and solvent were determined by means of the standard combination rule. PCM computations were carried out with standard parameters installed in the GAMESS program package.[15] (See ref 16 for the details of the parameters.) The nonelectrostatic contribution was semiempilically estimated by means of the Claverie−Pierotti method for cavitation energy[17] and by the Floris−Tomasi method for repulsion and dispersion free energy.[18] The Lennard-Jones formalism was used for the repulsion−dispersion contribution in which all of the parameters were taken to be the same as those in the RISM-SCF computations: the parameters of energy ($\epsilon$) and typical diameter ($\sigma$) were set for interaction between carbon−water oxygen, chlorine−water oxygen, and hydrogen−water oxygen.

The total energy of the solvation system is defined as the sum of the electronic energy of the solute ($E_{\text{solute}}$) and the solvation free energy ($\Delta\mu$).

$$\mathcal{A} = E_{\text{solute}} + \Delta\mu \tag{1}$$

$\Delta\mu$ contains all of the contributions from the solvent. The Fock operator ($F^{\text{solv}}$) contains a solvent-specific term,

$$F^{\text{solv}} = F^{\text{gas}} + V \tag{2}$$

$V$ expresses the solvent reaction field, which is the main difference between the two methods.

$$V^{\text{RISM-SCF}} = \rho \sum_{\lambda,\alpha} b_\lambda q_\alpha \int 4\pi r^2 \frac{g_{\lambda,\alpha}(r)}{r}\,\mathrm{d}r \qquad \text{(RISM-SCF)} \tag{3}$$

$$V^{\text{PCM}} = \sum_{i}^{\text{tesserae}} \frac{\sigma_i}{|\mathbf{r} - \mathbf{r}_i|} \qquad \text{(PCM)} \tag{4}$$

In eq 3, $\rho$ is the number of density, $b_\lambda$ is a population operator,[3] $g_{\lambda,\alpha}(r)$ is a pair correlation function between $\lambda$ (solute) and $\alpha$ (solvent), and $q_\alpha$ is the partial charge on the solvent site $\alpha$. $\sigma_i$ in eq 4 is the finite point charge placed in the middle of the surface tesserae. Note that even though both of them incorporate only the electrostatic interaction into the Fock operator the theoretical standpoints from which we deal with the solvation phenomena are very different between the two. Because the electronic structure of the solute and the solvation structure around it are determined in a self-consistent manner, the wave function of the solute molecule is distorted from that in the isolated state. The energy difference between the solute in the isolated state ($E_{\text{isolated}}$) and that in the solvent ($E_{\text{solute}}$) is a quantity used to measure the contribution of “solvation effects” to the electronic structure.

$$\begin{aligned} E_{\text{reorg}} &= E_{\text{solute}} - E_{\text{isolated}} \\ &= \langle\Psi|H|\Psi\rangle - \langle\Psi_0|H|\Psi_0\rangle \end{aligned} \tag{5}$$

where $|\Psi\rangle$ and $|\Psi_0\rangle$ are wave functions in solution and in the gas phase, respectively. $H$ is the electronic Hamiltonian of the molecule in the gas phase. $\mathcal{A}$ can be thus rewritten as the following:

$$\mathcal{A} = E_{\text{isolated}} + E_{\text{reorg}} + \Delta\mu \tag{6}$$

The RISM-SCF method compiles the ab initio electronic structure theory and statistical mechanical theory of molecular liquids. The solvation free energy in the present framework of the theory (excess chemical potential, $\Delta\mu_{\text{HNC}}$) is given by[19]

$$\Delta\mu_{\text{HNC}} = -\frac{\rho}{\beta}\sum_{\alpha s}\int \mathrm{d}\mathbf{r}\left[c_{\alpha s}(r) - \frac{1}{2}h^2_{\alpha s}(r) + \frac{1}{2}h_{\alpha s}(r)\,c_{\alpha s}(r)\right] \tag{7}$$

$h$ and $c$ are the total and direct correlation functions, respectively. $\beta = 1/k_BT$, where $k_B$ and $T$ are the Boltzmann constant and temperature, respectively. In PCM, the solvation free energy is evaluated with the sum of four separate contributions.

$$\Delta\mu_{\text{PCM}} = E_{\text{es}} + E_{\text{cav}} + E_{\text{dis}} + E_{\text{rep}} \tag{8}$$

where $E_{\text{es}}$, $E_{\text{cav}}$, $E_{\text{dis}}$, and $E_{\text{rep}}$ represent the electrostatic, cavitation, dispersion, and repulsion energy, respectively. This is the standard expression in the framework of PCM.[20]

## 3. Results and Discussion

Reaction energy profiles in the gas phase as well as PMF in aqueous solution are plotted in Figure 1. As is well known, the reaction barrier, which is 5.9 kcal/mol in the gas phase, is much higher in aqueous solution, and the ion−dipole complex, which is found in the gas phase at $R = 1.5$ Å, virtually disappears in aqueous solution. The energy changes obtained by the RISM-SCF and PCM methods are in excellent agreement: the barrier heights are 23.5 and 22.7 kcal/mol, respectively, and the profiles of PMF look very similar. A small difference between them is found around $R = 1.5$ Å, corresponding to the ion−dipole complex existing in the gas phase. Both of the curves are very close to those in the previous studies based on the RISM[10] and the molecular simulation calculations.[12] It is of great interest that the RISM-SCF, in which microscopic solvation is explicitly taken into account, and the PCM, in which an implicit treatment of the solvation is applied, provide very similar reaction profiles, at least from an energetic point of view.

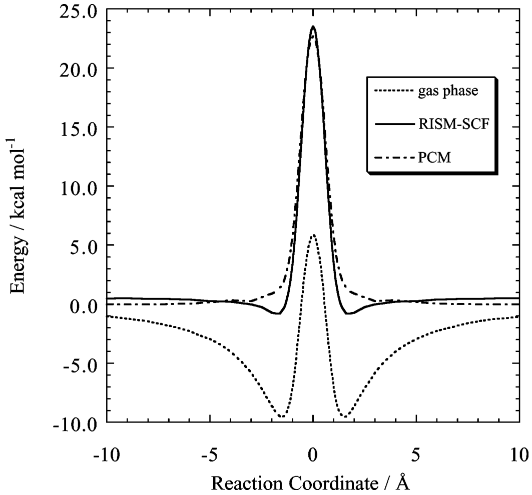

**Figure 1.** Comparison of PMF computed with RISM-SCF (—) and with PCM (— • —). The dashed line (- - -) is the gas-phase energy. All values are relative to the reactant given in Table 2.

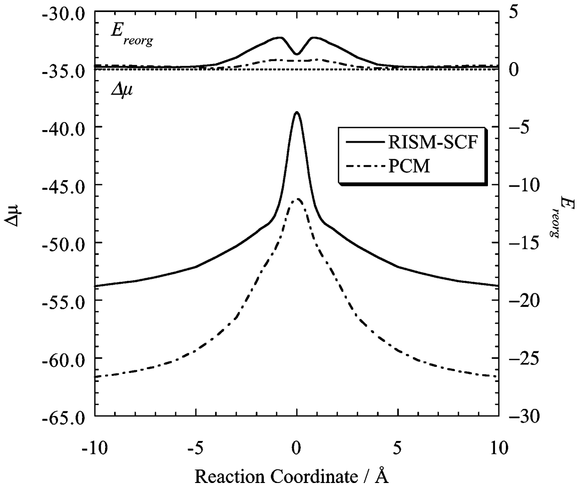

**Figure 2.** Two energy components, $E_{\mathrm{reorg}}$ and $\Delta\mu$, computed with RISM-SCF (—) and with PCM (— • —).

**TABLE 2: Energy Components**

| | gas | PCM | RISM-SCF |
|---|---|---|---|
| | $CH_3Cl$ | | |
| $E_{\mathrm{isolated}}{}^{a}$ | −499.13163 | | |
| $E_{\mathrm{reorg}}{}^{b}$ | | 0.48 | 0.32 |
| $\Delta\mu^{b}$ | | 2.30 | 15.21 |
| $A^{a}$ | | −499.12719 | −499.10688 |
| | $Cl^-$ | | |
| $E_{\mathrm{isolated}}{}^{a}$ | −459.56417 | | |
| $E_{\mathrm{reorg}}{}^{b}$ | | 0.04 | 0.00 |
| $\Delta\mu^{b}$ | | −65.16 | −70.63 |
| $A^{a}$ | | −459.66794 | −459.67672 |
| | $ClCH_3Cl^-$ ($R = 0$ Å) | | |
| $E_{\mathrm{isolated}}{}^{a}$ | −958.68642 | | |
| $E_{\mathrm{reorg}}{}^{b}$ | | 0.72 | 1.26 |
| $\Delta\mu^{b}$ | | −46.23 | −38.72 |
| $A^{a}$ | | −958.75895 | −958.74611 |

[a] Given in atomic units. [a] Given in kcal mol$^{-1}$.

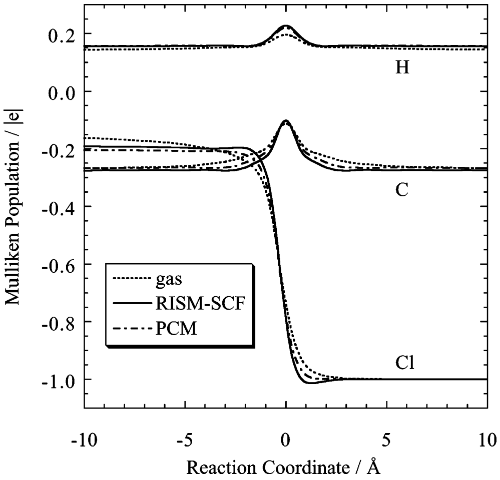

**Figure 3.** Mulliken charge population on each atom computed with RISM-SCF (—) and with PCM (— • —). The dotted line (• • •) is the gas-phase computation.

**3.1. Energy Components.** Figure 2 and Table 2 show the energy components, $\Delta\mu$ and $E_{\mathrm{reorg}}$, as functions of $R$. The profiles of $\Delta\mu$ computed by the two methods are very similar, although their absolute values are different by about 5.0 kcal/mol: Strong solvation is found both in the reactant and product, and stabilization due to solvation becomes weakest at $R = 0$ Å. As widely known, strong solvation due to hydrogen bonding between $Cl^-$ and the water solvent plays a significant role in the stabilization of the reactant and product states. The profile of $\Delta\mu$ in RISM-SCF is slightly narrower than that in PCM, suggesting that the solvation effect computed with RISM-SCF is suddenly changed around $R = -3$ to 3 Å. The aforementioned disagreement in the absolute values of the solvation energies can be attributed to several sources. For example, we adopt the Claverie−Pierotti method for $E_{\mathrm{cav}}$ in the present study, which gives about 13 kcal/mol (13.0 kcal/mol at $R = 0$ Å and 13.8 kcal/mol at $R = \pm 10.0$ Å). The value becomes ca. 8 kcal/mol if we use the Pierotti method based on a single sphere. However, it should be noted that the difference in absolute values is systematically removed when we see the reaction as the relative energy with respect to the reactant (or product). $\Delta\Delta\mu = \Delta\mu(R = 0\text{Å}) - \Delta\mu(\text{reactant}, R = -\infty)$ is 16.70 kcal/mol by RISM-SCF and 16.63 kcal/mol by PCM, strongly indicating that the disagreement in the absolute value of $\Delta\mu$ is not essential to our understanding of the reaction.

$E_{\mathrm{reorg}}$ is alway positive because of the nature of the wave function determined by the variational principle, and it is much smaller than $\Delta\mu$ in the present system. $E_{\mathrm{reorg}}$ is less than 3 kcal/mol in RISM-SCF and less than 1 kcal/mol in PCM. It is interesting that $E_{\mathrm{reorg}}$ computed with RISM-SCF shows a dip around $R \approx 0$ Å and that $E_{\mathrm{reorg}}$ with PCM is very flat and broad over a wide range of $R$. The difference in $E_{\mathrm{reorg}}$ between the two methods, namely, the difference in the wave functions, can be attributed to the difference in the strength of solvation around $R = 1.5$ Å. Greater $E_{\mathrm{reorg}}$ in RISM-SCF could be attributed to strong solvation compared to that in PCM around this region. Note that this shares the view of the aforementioned difference in the profile of $\Delta\mu$. As we shall return to this point below, the difference is also consistent with the change in the pair correlation function along $R$. Although the overall features of PMF in the two methods, which are determined with the sum of $\Delta\mu$ and $E_{\mathrm{reorg}}$, are very similar as we have shown in Figure 1, the physicochemical background of the reaction profiles seems to be slightly different.

**3.2. Change in Electronic Structure at the Atomic Level.** One of the traditional ways to understand the change in electronic structure along the chemical reaction is to analyze the Mulliken charge population. Figure 3 plots the Mulliken charge of composing atoms as functions of $R$, which are computed with standard MO (gas-phase), RISM-SCF, and PCM methods. Only the leaving Cl atom of the two is shown here because the approaching Cl atom is shown upon going from right to left. The charge distributions obtained both by RISM-SCF and PCM computations are more polarized than those obtained by gas-phase computations. The PCM results are intermediate between RISM-SCF and gas-phase results. Remarkable differences in the charge distribution of the H atom is found around $R = 0$ Å, but the deviation from the gas-phase charge distribution in the C atom is found over a wide range of the reaction coordinate except for $R = 0$ Å. The atomic population of Cl in $CH_3Cl$ is different between gas and solution phases because of the polarization ($R < 0$), but the value in solution quickly becomes identical to that in the gas phase ($q_{Cl} = -1$) upon leaving the $CH_3$ group ($R > 3$Å). In aqueous solution, the H atom becomes more positively charged, and the Cl and C atoms become more negatively charged around $R \approx 0$ than those in gas phase, suggesting that the solvation induces polarization in the $CH_3$ group as well as enhancing the charge transfer from the $CH_3$ group to the leaving Cl. The effect is slightly greater in RISM-SCF than in PCM, and a little charge overshooting is observed in RISM-SCF. This is caused by a specific enhancement of hydrogen bonding, as we will discuss below.

We wish to present a more detailed discussion from an energetic point of view by introducing an energy-partitioning scheme. The electronic energy and its distortion ($E_{\mathrm{reorg}}$) from the wave function in the gas phase can be "formally" partitioned into the contribution from the composite atoms by using the recently proposed procedure.[21,22] The energy partitioned on atom α is given by eq 9. (See ref 22 for details.)

$$\begin{aligned} E^{\alpha} = & \sum_{\nu\in\alpha}\sum_{\mu} P_{\nu\mu}\left\langle \mu \left| -\frac{1}{2}\nabla^2 \right| \nu \right\rangle \\ & + \frac{1}{2}\sum_{\nu\in\alpha}\sum_{\mu} P_{\nu\mu}\left\langle \mu \left| \sum_{A}\frac{Z_A}{r_A} \right| \nu \right\rangle \\ & + \frac{1}{2}\sum_{\nu}\sum_{\mu} P_{\nu\mu}\left\langle \mu \left| \frac{Z_\alpha}{r_\alpha} \right| \nu \right\rangle \\ & + \frac{1}{2}\sum_{\nu\in\alpha}\sum_{\mu} P_{\nu\mu}G_{\mu\nu} + \frac{1}{2}\sum_{B\neq\alpha}\frac{Z_\alpha Z_B}{R_{\alpha B}} \end{aligned} \tag{9}$$

The energy-partitioning scheme shown here is analogous to the Mulliken population analysis and is a way to define the local energy assigned to each composing atom.

We compute the total energy of molecules in the gas and solution phases, in which the partitioned energies are defined as follows:

$$\begin{aligned} E_{\mathrm{solute}} &= \sum_{\alpha} E^{\alpha}_{\mathrm{solute}} \\ E_{\mathrm{isolated}} &= \sum_{\alpha} E^{\alpha}_{\mathrm{isolated}} \end{aligned} \tag{10}$$

The difference between these energies corresponds to the partitioned reorganization energy.

$$E_{\mathrm{reorg}} = \sum_{\alpha} E^{\alpha}_{\mathrm{reorg}} = \sum_{\alpha}(E^{\alpha}_{\mathrm{solute}} - E^{\alpha}_{\mathrm{isolated}}) \tag{11}$$

This quantity represents how much the local (atomic level) electronic structure of the solute is affected by solvation.

Figure 4 represents the partitioned energy of each atom in the gas phase. All of the energies are relative values with respect to those in the reactant. Note that the sum of all of these components equals the gas-phase potential energy shown in Figure 1. These relative energies show long-range behavior, and all of them gradually decrease to zero around $|R| = 20$ Å. The partitioned energy is considered to represent the electronic structure in individual atoms. Roughly speaking, a decrease (increase) in energy indicates a loss (gain) of electrons at the specific atom. A similar discussion has been included in a conceptual study of density functional theory. The partitioned energies of H atoms in $CH_3Cl$ and that of the approaching Cl (dashed line in the figure) show a minimum around $R = -1.5$ Å, indicating that the contribution from these atoms stabilizes the ion−dipole complex. The electronic structure of Cl bound to the $CH_3$ group (solid line) is not affected very much at the beginning of the reaction ($R \approx -1.5$Å) but suddenly changes after passing through the complex ($R \approx 0$). Because the contribution from two Cl atoms is negative, the origin of the barrier of the $S_N2$ reaction is attributed to the destabilization of C and H atoms, which is caused by losing electrons. This may also concern the change in bonding structure from $sp^3$ (ion-dipole complex) to $sp^2$ ($R = 0$ Å), namely, the enhancement of a resonance structure of $Cl^-[CH_3]^+Cl^-$ at $R = 0$ Å. This is consistent with the previous computations based on MOVB and VBSCF.[9] As $Cl^-$ leaves (solid line in $R > 0$), the polarization of C−H bonds in $CH_3Cl$ gradually decreases. However, $E^{\mathrm{Cl}}_{\mathrm{isolated}}$ (dashed line in $R > 0$) is almost constant, which means that the electronic structure of the Cl atom in $CH_3Cl$ is not affected by the electric field generated by the leaving $Cl^-$.

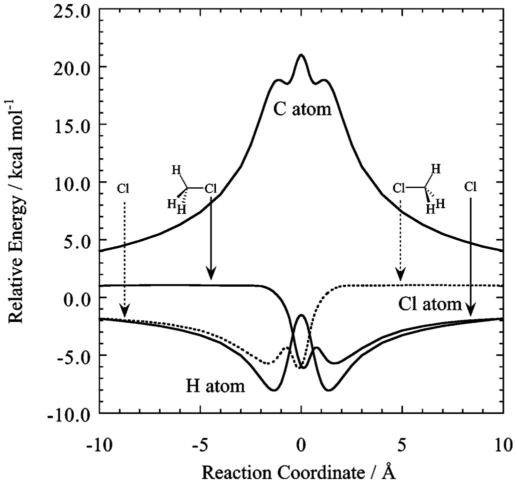

**Figure 4.** Partitioned energy on each atom ($E^{\alpha}$) obtained by the gas-phase computation. Changes in C, H, and Cl atoms are plotted. The leaving Cl atom (right-hand side of the illustrated molecule) is represented by a solid line, and the other Cl atom is represented by a dotted line. The profile of the H atom appears below.

Because the behaviors of the partitioned energies in aqueous solution are similar to those in the gas phase, only the deviation from the gas-phase value ($E^{\alpha}_{\mathrm{reorg}}$) is plotted in Figure 5. Note that the scale of the vertical axis in the figure is much smaller than that in Figure 4. The upper panel of the figure shows the energy contribution from the leaving Cl atom corresponding to the solid line in Figure 4. In the region of $R < 0$ (Cl is bound to the $CH_3$ group), $E^{\mathrm{Cl}}_{\mathrm{reorg}}$ is negative, indicating that the Cl atom attracts an electron from the $CH_3$ group to a greater extent than that in the gas phase. This polarization in the PCM wave function is slightly greater than that in the RISM-SCF wave function, and both of them are monotonically weakened when approaching the point $R = 0$. RISM-SCF calculations show that $E^{\mathrm{Cl}}_{\mathrm{reorg}}$ at $R = 1.5$ Å deviates greatly from that in the gas phase. Because the ion−dipole complex is found around this region

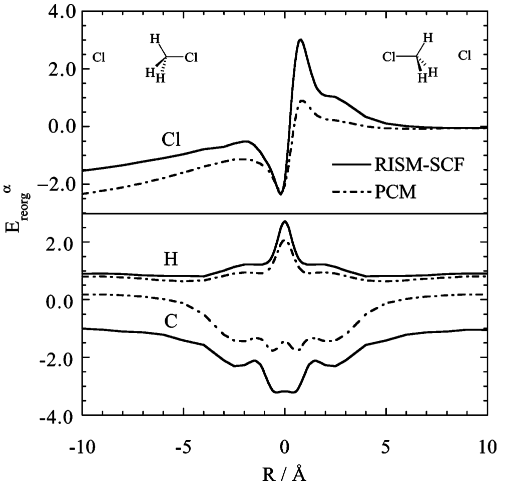

**Figure 5.** Partitioned reorganization energy on each atom ($E^{\alpha}_{\text{reorg}}$) computed with RISM-SCF (—) and with PCM (— • —). The upper panel shows the energy change in Cl atoms. (The leaving Cl atom corresponding to the solid line in Figure 4.) The lower panel shows H (upper two lines) and C (lower two lines) atoms.

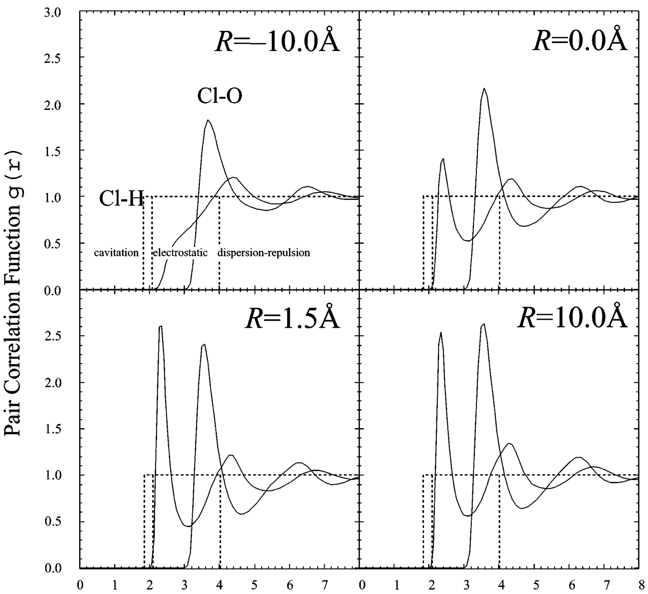

**Figure 6.** Solvation structure obtained from RISM-SCF along the reaction. The step functions (• • •) indicate the size of the cavity in PCM.

of $R$, the deviation is attributed to the enhancement of stabilization in the ion−dipole complex due to polarization. When $Cl^-$ leaves ($R > 0$), the polarization in RISM-SCF is greater than that in PCM and shows rapid convergence to the electronic structure of the gas phase. In C and H atoms, the RISM-SCF method always gives greater polarization than does the PCM method (lower panel). These results suggest that the bond polarization of $Cl-CH_3$ is enhanced in the wave function obtained by PCM whereas that of C−H is also important in the wave function obtained by RISM-SCF. One may notice that the dip found in $E_{\text{reorg}}$ in Figure 2 could relate to the change in the electronic structure of the Cl atoms.

**3.3. Solvation Structure.** Although the prediction capability for the total energy seems very similar in the RISM-SCF and PCM methods, a considerable difference between them concerns the information of microscopic solvation. The solvation structure is described in terms of a set of pair correlation functions (PCFs) in the RISM-SCF theory. Shown in Figure 6 is the PCFs of solvent water molecules around Cl, corresponding to the leaving atom plotted as a solid line in Figure 4. In the reactant, the Cl atom is bound to the $CH_3$ group, and there is no hydrogen bonding. As the reaction goes through $R = 0$ to the product, a sharp peak located around 2 Å grows up. This peak corresponds to hydrogen bonding. It is noted that the peak height in $R = 1.5$ Å is slightly higher than that in $R = 10.0$ Å. This behavior is consistent with the charge overshooting that occurs in the ion−dipole complex. The PCM does not provide any information on the solvation structure: it can be regarded as a model in which the distribution function is approximated with a step function, $\theta(R - R_0)$:

$$g(R) \approx \theta(R - R_0) = \begin{cases} 0 & R \le R_0 \\ 1 & R > R_0 \end{cases}$$

This means that a solvent molecule never exists inside the cavity boundary ($R \le R_0$) and that the continuum distribution (without any solute−solvent correlation) is defined outside the boundary ($R > R_0$). The treatment of the solvent distribution in PCM is essentially based on a description of long-range (“macroscopic”) interaction. This is consistent with the fact that all of $g(r)$ in RISM-SCF converges to unity as increasing $R$. In the theory, three different representative lengths corresponding to the individual contribution in eq 8 are used to define the size of the cavity (radius, $R_0$) (i.e., electrostatic, cavitation, and dispersion−repulsion, as shown in the figure). See ref 16 for details of these radii. It is interesting that the boundary of the cavity is generally close to the rise of the peak in $g(r)$. The radius representing the electrostatic interaction coincides with the rise of $g(r)$ between H and Cl, which is actually the hydrogen bonding. At the same time, this interaction determines the spatial arrangement between the solute and solvent and relates to the cavitation. The interaction between electron-rich atoms, O−Cl, may be concerned with the dispersion−repulsion interaction. The essential difference in the distribution functions between the two methods is their probability: the above-mentioned subtle difference found in PMF between the two methods relies on the strength of solvation (i.e., the height of the distribution function), which describes the probability. From a coarse-grained (long-range) viewpoint, the progress of the $S_N2$ reaction is regarded as charge shifting along the molecular axis of Cl−C−Cl. This may be the reason that the polarization of the Cl−C bond is enhanced in the electronic structure obtained by PCM. Similar polarization is found in RISM-SCF; however, the polarization of the C−H bond is also emphasized. The polarization in RISM-SCF is caused by a local (or microscopic) interaction between the methyl hydrogen and the solvent water oxygen ($g_{H-O}(r)$ is not shown here), which consequently weakens the polarization of C−Cl. Thus, the small difference found in PMF could be attributed to the difference in the microscopic description of the solvation structure. Because the height of peak and the electronic structure in the solute are strongly coupled to each other, further careful investigation is necessary to describe chemical processes in solution properly.

## 4. Conclusions

Electronic structures of solvated molecule are computed within the framework of modern two methods—RISM-SCF and PCM—and critically compared. Two different methods provide very similar energy profiles of $S_N2$ reaction, though the energy components are slightly different between the two methods: The electronic distortion due to solvation ($E_{\text{reorg}}$) obtained by PCM is slightly smaller than that obtained by RISM-SCF. A detailed analysis based on the energy partitioning in atomic level reveals that the bond polarization of Cl−$CH_3$ is enhanced in the wave function obtained by PCM whereas that of C−H is also important in the wave function obtained by RISM-SCF.

We emphasize that even in a situation in which the computational energy is almost identical there could still be a difference in the description of chemical phenomena such as the solvation structure. Further careful analysis and continuous efforts to develop more sophisticated methods are highly desired to clarify the true process in the real solution system.

**Acknowledgment.** This research was supported by a Grant-in Aid for Encouragement of Young Scientists and by the Japanese Ministry of Education, Science, Sports and Culture (MONBU SHO).

## References and Notes

(1) (a) *Computational Biochemistry and Biophysics*; Becker, O. M., MacKerell, A. D., Jr., Roux, B., Watanabe, M., Eds.; Marcel Dekker: New York, 2001. (b) *Combined Quantum Mechanical and Molecular Mechanical Methods*; ACS Symposium Series 712; American Chemical Society: Washington, DC, 1998. (c) Cramer, C. J.; Truhlar, D. G *Chem. Rev*. **1999**, *99*, 2161. (d) Orozco, M.; Luque, F. *Chem. Rev*. **2000**, *100*, 4187.

(2) (a) Miertus, S.; Scrocco, E.; Tomasi, J. *Chem. Phys*. **1981**, *55*, 117. (b) Tomasi, J.; Persico, M. *Chem. Rev*. **1994**, *94*, 2027.

(3) Ten-no, S.; Hirata, F.; Kato, S. *J. Chem. Phys*. **1994**, *100*, 7443.

(4) Sato, H.; Hirata, F.; Kato, S. *J. Chem. Phys*. **1996**, *105*, 1546.

(5) Chandler, D.; Andersen, H. C. *J. Chem. Phys*. **1972**, *57*, 1930.

(6) (a) Hirata, F.; Rossky, P. J. *Chem. Phys. Lett*. **1981**, *83*, 329. (b) Hirata, F.; Pettitt, B. M.; Rossky, P. J. *J. Chem. Phys*. **1982**, *77*, 509. (c) Hirata, F.; Rossky, P. J.; Pettitt, B. M. *J. Chem. Phys*. **1983**, *78*, 4133.

(7) (a) Bianco, R.; Miertuš, S.; Persico, M.; Tomasi, J. *Chem. Phys*. **1992**, *168*, 281. (b) Aguilar, M.; Bianco, R.; Miertuš, S.; Persico, M.; Tomasi, J. *Chem. Phys*. **1993**, *174*, 397. (c) Pomelli, C. S.; Tomasi, J. *J. Phys. Chem. A* **1997**, *101*, 3561.

(8) Ruiz-López, M. F.; Rinaldi, D.; Bertrán, J. *J. Chem. Phys*. **1995**, *103*, 9249.

(9) Mo, Y.; Gao, J. *J. Comput. Chem*. **2000**, *21*, 1458.

(10) Huton, S. E.; Rossky, P. J.; Zichi, D.A. *J. Am. Chem. Soc*. **1989**, *111*, 5680.

(11) Van der Zwan, G.; Hynes, J. *J. Chem. Phys*. **1983**, *78*, 4174.

(12) (a) Chandrasekhar, J.; Smith, S. F.; Joregensen, W. L. *J. Am. Chem. Soc.* **1984**, *106*, 3049. (b) Chandrasekhar, J.; Smith, S. F.; Joregensen, W. L. *J. Am. Chem. Soc.* **1985**, *107*, 154. (c) Chandrasekhar, J.; Joregensen, W. L. *J. Am. Chem. Soc.* **1985**, *107*, 2974.

(13) Krishnan, R.; Binkley, J. S.; Seeger, R.; Pople, J. A. *J. Chem. Phys*. **1980**, *72*, 650.

(14) Sato, H.; Hirata, F. *J. Am. Chem. Soc*. **1999**, *121*, 3460.

(15) Schmidt, M. W.; Baldridge, K. K.; Boatz, J. A.; Elbert, S. T.; Gordon, M. S.; Jensen, J. J.; Koseki, S.; Matsunaga, N.; Nguyen, K. A.; Su, S.; Windus, T. L.; Dupuis, M.; Montgomery, J. A. *J. Comput. Chem.* **1993**, *14*, 1347.

(16) Parameters used in the PCM computations are as follows: cavity radii for C are 2.04, 1.70, and 3.085 Å corresponding to electrostatic, cavitation, and dispersion−repulsion terms, respectively. Values for Cl are 2.172, 1.81, and 3.195 Å, and those for H are 1.44, 1.20, and 2.585 Å, respectively. The cavitation energy reported by Pierotti and Claverie is computed with standard values: 78.39 (dielectric constant), 1.776 (dielectric constant at infinite frequency), 18.07 mL/mole (molecular volume), 0.000257 $K^{-1}$ (thermal expansion coefficient), 71.81 dyn/cm (surface tension), 0.65 (thermal coefficient of log(thermal expansion coefficient)), 1.277 (cavity microscopic coefficient), and 1.385 Å (solvent radius). Repulsion and dispersion energies were computed with the empirical method of Floris and Tomasi using atom−atom interaction through the Lennard-Jones-type potential. The same parameters in the RISM-SCF computations were used. The solvent parameters are substituted by those of the water oxygen.

(17) Langlet, J.; Claverie, P.; Caillet, J.; Pullman, A. *J. Phys. Chem*. **1988**, *92*, 1617.

(18) Floris, F.; Tomasi, J. *J. Comput. Chem*. **1989**, *10*, 616.

(19) Singer, S. J.; Chandler, D. *Mol. Phys*. **1985**, *55*, 621.

(20) Barone, V.; Cossi, M.; Tomasi, J. *J. Chem. Phys*. **1997**, *107*, 3210.

(21) Nakai, H. *Chem. Phys. Lett*. **2002**, *363*, 73.

(22) Sato, H.; Hirata, F.; Sakaki, S. *J. Phys. Chem. A*, in press.